

## VALIDATION OF A COMPUTATIONAL MODEL FOR A COUPLED LIQUID AND GAS FLOW IN MICRO-NOZZLES

R. Zahoor<sup>1\*</sup>, J. Knoška<sup>2,3</sup>, J. Gregorc<sup>1</sup>, S. Bajt<sup>4</sup> and B. Šarler<sup>1,5</sup>

<sup>1</sup>Laboratory for Fluid Dynamics and Thermodynamics,  
Faculty of Mechanical Engineering, University of Ljubljana,  
Aškerčeva 6, 1000 Ljubljana, Slovenia

E-mail: rizwan.zahoor@fs.uni-lj.si, jurij.gregorc@fs.uni-lj.si, bozidar.sarler@fs.uni-lj.si

<sup>2</sup>Center for Free Electron Laser Science, DESY,  
Notkestraße 85, 22607 Hamburg, Germany

<sup>3</sup>Dept. Physics, University of Hamburg,  
Luruper Chaussee 149, 22761 Hamburg, Germany  
E-mail: juraj.knoska@desy.de

<sup>4</sup>Deutsches Elektronen-Synchrotron DESY,  
Notkestraße 85, 22607 Hamburg, Germany  
E-mail: sasa.bajt@desy.de

<sup>5</sup>Laboratory for Simulation of Materials and Processes,  
Institute of Metals and Technology,  
Lepi pot 11, 1000 Ljubljana, Slovenia  
E-mail: bozidar.sarler@imt.si

**Key words:** Gas Dynamic Virtual Nozzle, Micro-Jet, Jet Shape, Jet Velocity, Coupled Numerical Model.

**Abstract.** The work presents verification of a numerical model for micro-jet focusing, where a coupled liquid and gas flow occurs in a gas dynamic virtual nozzle (GDVN). Nozzles of this type are used in serial femtosecond crystallography experiments to deliver samples into X-ray beam. The following performance criteria are desirable: the jet to be longer than 100  $\mu\text{m}$  to avoid nozzle shadowing, the diameter as small as possible to minimize the background signal, and the jet velocity as high as possible to avoid sample's double X-ray exposure. Previous comprehensive numerical investigation has been extended to include numerical analysis of the tip jet velocities. These simulations were then compared with the experimental data. The coupled numerical model of a 3D printed GDVN considers a laminar two-phase, Newtonian, compressible flow, which is solved based on the finite volume method discretization and interface tracking with volume of fluid (VOF). The numerical solution is calculated with OpenFOAM based compressible interFoam solver, which uses algebraic formulation of VOF. In experimental setup for model validation a 3D printed GDVN was inserted in a vacuum chamber with two windows used for illumination and visualization. Once the jet was stabilized

its velocity was estimated based on a distance a droplet traveled between two consecutive illumination pulses with a known time delay. The experimental and computational study was performed for a constant liquid flow rate of 14  $\mu\text{l}/\text{min}$  and the gas mass flow rate in the range from 5 mg/min to 25 mg/min. The coupled numerical model reasonably predicts the jet speed and shape as a function of the gas flow.

## 1 INTRODUCTION

Liquid micro-jets are efficient vectors of mass and momentum, which find applications in countless scientific domains, most recently in serial femtosecond crystallography (SFX) [1]. In SFX they are used as sample carriers for beam interactions, where diffraction patterns of these samples are collected as they interact with femtosecond X-ray pulses from X-ray Free-Electron Lasers (XFELs). These crystal samples are very small with typical dimensions of sub- to few microns and their weak scattering ability requires very high-intensity X-ray beams to produce a sufficient signal for meaningful data collection. The samples are delivered into X-ray beam via a liquid jet, thus some characteristics of the carrier jet are of utmost importance, such as its diameter, length and velocity. The diameter of the jet should be as small as possible to increase the signal of the sample relative to the background from the buffer liquid. In addition, the jet has to be long enough so that the interaction with X-ray beam can be far enough from the nozzle to avoid any shadowing from the nozzle structure in the X-ray diffraction data. The interaction of the jet with the X-ray is normally carried out at a distance of  $\sim 100$   $\mu\text{m}$  or more. The X-ray beams coming out from XFELs operate with a frequency of 120 Hz (e.g. LCLS) or as high as 4.5 MHz (e.g. European XFEL). In order to avoid a double exposure of the crystal the jet has to be as fast as possible. For biological samples it is also important to know the temperature of the jet.

Liquid jets are produced in many ways starting from Rayleigh sources [2], to more recently, gas dynamic virtual nozzles (GDVNs) [3]–[6]. Rayleigh sources are inefficient for SFX applications because of their limitations in producing fast, micron/sub-micron jets [5]. To overcome these issues, a novel way of producing liquid jets was introduced using a hydrodynamic effect of the co-flowing gas stream [3]. Further improvement was to replace the plate with an orifice with a glass polished converging outer capillary [4]. This increased the harvesting of the focusing moment from the co-flowing gas. An injection molded GDVN [5] was introduced to overcome manufacturing difficulties in glass polished nozzles. More recently 3D printed GDVNs [7] were introduced, enabling advanced micro-nozzle design solutions and manufacturing with high accuracy and reproducibility.

As the jet emanates from nozzle outlet in provided environment various instabilities co-exist on the jet surface. These instabilities determine the jet characteristics, which are either (a) an unstable meniscus with periodic ejection of drops - dripping, (b) a continuous stable liquid thread, which finally breaks into stream of droplets - jetting, (c) spatially unstable jet, which whips with some amplitude - whipping [3], [8]. There are various strongly coupled factors that result in the jet outcome (jetting/dripping/whipping). They include nozzle geometry, liquid and gas operating parameters, gas and liquid material properties.

Numerical simulations have become very successful in studying the jet characteristics. They have been performed for jet emanating in air [9], [10] and vacuum environments [6], [11], [12]. Recently, the jet characteristics have been investigated for injection molded GDVNs using

experimentally validated numerical model for a wide spectrum of liquid and gas flow rates [6], nozzle geometry [11] and type of focusing gas [12].

Present work extends these numerical investigations by using the same numerical model as in [6] for the assessment of the jet speed as a function of gas flow rate for a 3D printed nozzle. A fixed nozzle geometric arrangement is used for numerical study, where the numerical results are compared with the experimentally collected data. The numerical formulation is followed with the short description of governing equations and the basics of the solution procedure. Numerical results are discussed for 5 different cases where the liquid flow rate is kept constant, while the gas flow is changed. Conclusions are drawn in the final section based on the results of the numerical model and its comparison with the related experiment.

## 2 METHODOLOGY

In this experiment we attempted to collect the jet length, diameter and the velocity of a 3D printed GDVN. The same experimental setup as in [5] was used. However, this time also the jet speed was recorded by using two laser pulses with a known delay. The distance travelled by the first drop detaching from the jet tip was recorded and the speed was measured.

Numerical domain of GDVN used for numerical simulation is shown in **Figure 1**. The GDVN geometry has a cylindrical symmetry so an axisymmetric modelling approach is applied instead of a full 3D modelling. The numerical model, including the boundary conditions used along with the solution setup are elaborated in [6]. Only basic elements of the numerical model are summarized in the present paper.

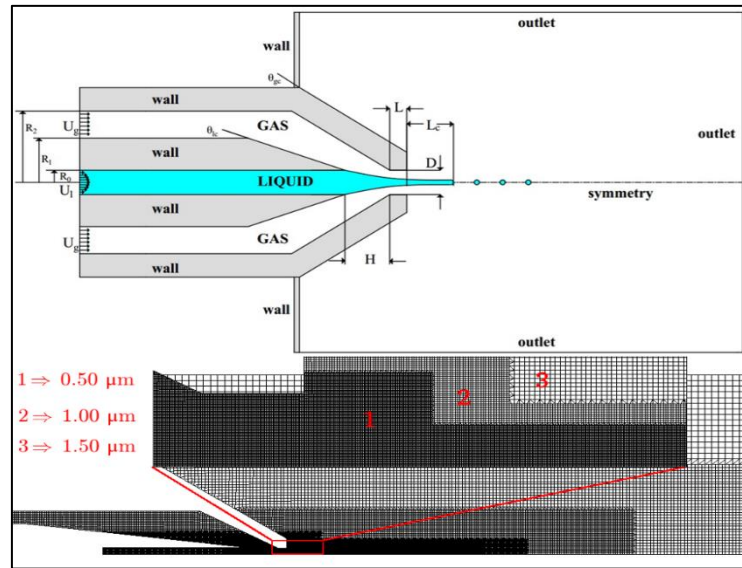


**Figure 1.** Schematic of GDVN used for numerical simulations (not to scale), where  $R_2 = 25 \mu\text{m}$ ,  $R_1 = 70 \mu\text{m}$ ,  $R_2 = 175 \mu\text{m}$ ,  $H = 60 \mu\text{m}$  and  $D = 60 \mu\text{m}$ .

A single-domain VOF approach includes a volume fraction variable  $\alpha(\mathbf{p}, t)$ , bounded between 0 and 1 for gas and liquid, respectively. The interface transport equation along with the mixture formulation of coupled mass, momentum and energy equations are given as follows,

$$\partial(\rho\alpha)/\partial t + \nabla \cdot (\rho \mathbf{v} \alpha) = 0 \quad (1)$$

$$\partial\rho/\partial t + \nabla \cdot (\rho \mathbf{v}) = 0, \quad (2)$$

$$\partial(\rho \mathbf{v})/\partial t + \nabla \cdot (\rho \mathbf{v} \mathbf{v}) = -\nabla p + \nabla \cdot \bar{\boldsymbol{\tau}} + \mathbf{f}_\sigma \quad (3)$$

$$\partial(\rho e)/\partial t + \nabla \cdot (\rho \mathbf{v} e) = -\nabla \cdot (\rho \mathbf{v}) + \nabla \cdot (\bar{\boldsymbol{\tau}} \mathbf{v}) - \nabla \cdot \mathbf{q} \quad (4)$$

where  $\mathbf{v}(\mathbf{p}, t)$  is velocity vector and  $\rho$  is density,  $p(\mathbf{p}, t)$  denotes pressure,  $\mathbf{f}_\sigma(\mathbf{p}, t)$  surface tension forces,  $\bar{\boldsymbol{\tau}}$  the viscous stress tensor, defined as  $\bar{\boldsymbol{\tau}} = \mu [(\nabla \mathbf{v}) + (\nabla \mathbf{v})^T] - \lambda (\nabla \cdot \mathbf{v}) \mathbf{I}$  with viscosity  $\mu$ ,  $\lambda = (2/3)\mu$  and identity tensor  $\mathbf{I}$ , while  $e$  is the specific total energy per unit volume, composed from the specific internal and the kinetic energy per unit volume  $e = c_v T + 0.5 |\mathbf{v}|^2$  with  $c_v$  and  $T$  standing for specific heat capacity at constant volume and temperature respectively,  $\mathbf{q} = -k \nabla T$  is the conduction heat flux with thermal conductivity  $k$ . The material properties satisfying equations (1) - (4) are calculated from the phase-weighted averages as,

$$\mathcal{G}(\alpha) = \alpha \mathcal{G}_l + (1 - \alpha) \mathcal{G}_g, \quad (5)$$

where,  $\mathcal{G}_l$  and  $\mathcal{G}_g$  stand for the liquid and gas material properties, such as density, specific heat, thermal conductivity and viscosity. Ideal gas is considered for density calculation.

The high speeds and micro-dimensionality of the nozzle system allow to neglect the gravitational force. The dominant surface tension force is included as the body force  $\mathbf{f}_\sigma = \sigma \kappa \mathbf{n}$ , with  $\sigma$  standing for surface tension,  $\mathbf{n} = \nabla \alpha$  is the unit normal and the curvature of the interface calculated by using the continuum surface model [13] as,  $\kappa(\alpha) = -\nabla \cdot (\nabla \alpha / |\nabla \alpha|)$ .

Numerical simulations are performed with OpenFOAM code [14], which is based on FVM discretization. The liquid-gas interface is captured with VOF method, where the interface diffusion is avoided by using an artificial interface compression counter-gradient approach [15]. PIMPLE algorithm is used for the solution of partial differential equations and an adaptive time stepping approach is used by setting [16] Courant number  $Co = (|\mathbf{v}| \Delta t / \Delta x)$  equal to 0.25.

### 3 RESULTS AND DISCUSSIONS

Numerical simulations were done for a set of 5 different helium gas flow rates (5 mg/min, 10 mg/min, 15 mg/min, 20 mg/min and 25 mg/min), and where the water flow rate was kept constant at 14  $\mu\text{l}/\text{min}$ . The jet diameter, length and velocity were analyzed as a function of the gas flow rate. Experimental data was extracted and compared with the numerical simulations in terms of jet length, diameter and velocity in **Figure 2, 3 and 4**.

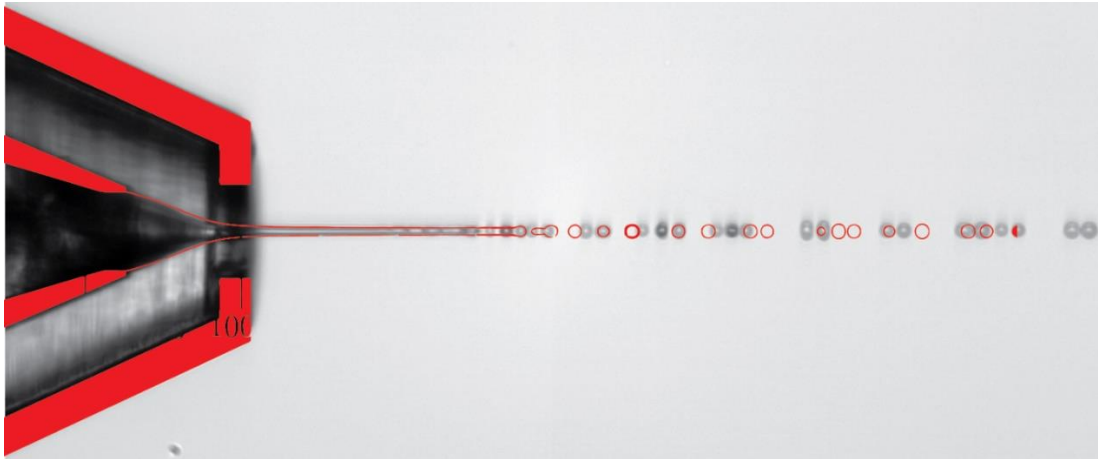


**Figure 2.** Comparison of the numerical (red) and experimental (black) jet shape for a liquid and gas flow rate of  $14 \mu\text{l}/\text{min}$  and  $5 \text{ mg}/\text{min}$ , respectively.

It is seen from the jet snapshots in **Figure 2**, that the jet shape obtained with the numerical simulation reasonably agrees with the experimental one. To analyze the data, the jet shape was averaged over time, once the simulation was stabilized. These time averaged values are presented in **Figure 3 - (a, b)**.

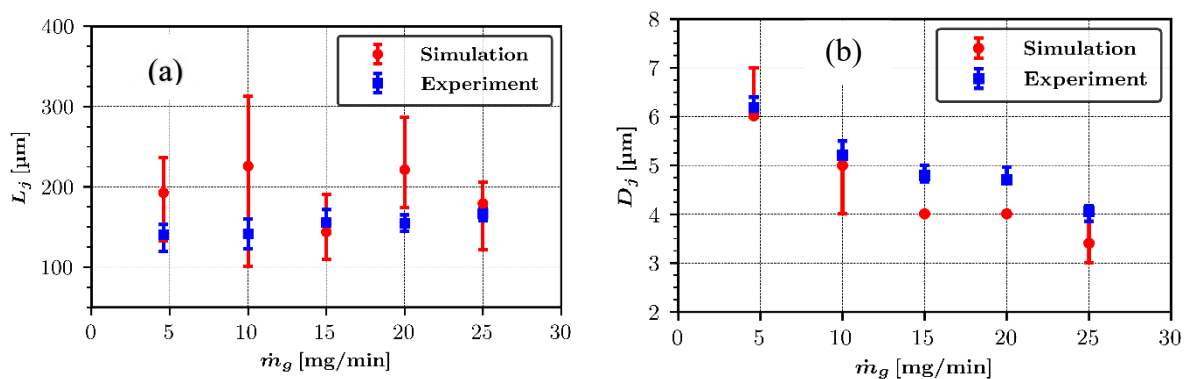


**Figure 3.** Numerical and experimental (a) jet length and (b) jet diameter for a liquid flow rate  $14 \mu\text{l}/\text{min}$  and 5 different gas flow rates.

Experimentally measured velocities and velocities obtained from numerical simulations are presented in **Figure 4**. It is interesting to note a consistent underestimation of the calculated jet velocities as compared to the experimentally measured ones. This difference could potentially be explained with how these velocities were measured. In the experimental setup the velocity of the first detached drop from the jet is monitored as it moves downstream in the nozzle outlet chamber. In the numerical simulations we are extracting the velocity of the tip of the jet. The first detached drop accelerates in high speed gas stream co-flowing with the jet causing the difference in velocity comparison.

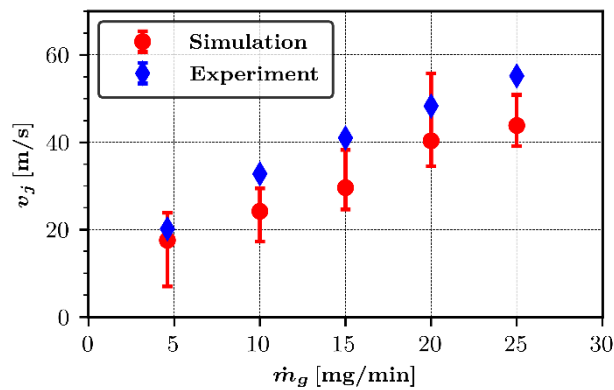


**Figure 4.** Numerical and experimental jet velocity for a liquid flow rate  $14 \mu\text{l}/\text{min}$  and for 5 different gas flow rates.

#### 4 CONCLUSIONS

The FVM-VOF based numerical model was used to assess the jet focusing for a 3D printed micro GDVN. The measured and calculated jet shapes show reasonable agreement. However, simulated velocities are consistently slower than experimentally measured ones, this difference could possibly be introduced by the velocity measurement. In the experiments we measure the velocity of the first detached drop from the jet, because measuring the velocity closer to the tip of the jet was not possible. Similarly, in numerical simulations it is not easily possible to retrieve velocities of the first detached drop. A more accurate comparisons would require assessing flow characteristics of the jet at same position. In spite of the discrepancies present in measured and calculated velocities, the study overall provides a good way forward for future such investigations. In the numerical simulations there are no such constrains and we can easily retrieve the velocity of the tip of the jet.

#### 5 ACKNOWLEDGMENTS

Funding for this research is provided by the Centre of Free Electron Laser (CFEL) under project: Innovative methods for imaging with the use of X-ray free electron laser (XFEL) and synchrotron sources: simulation of gas-focused micro-jets, and Slovenian Grant Agency (ARRS) within Program Group P2-0162 and Project J2-7384. The computations were performed on high performance computational resources at Faculty of Mechanical Engineering, University of Ljubljana.

## REFERENCES

- [1] H. N. Chapman *et al.*, “Femtosecond X-ray protein nanocrystallography,” *Nature*, vol. 470, no. 7332, pp. 73–77, Feb. 2011.
- [2] L. Rayleigh, “On the instability of jets,” *Proc. Lond. Math. Soc.*, vol. 10, pp. 4–13, 1878.
- [3] A. M. Gañán-Calvo, “Generation of steady liquid microthreads and micron-sized monodisperse sprays in gas streams,” *Phys. Rev. Lett.*, vol. 80, no. 2, pp. 285–288, Jan. 1998.
- [4] D. P. DePonte *et al.*, “Gas dynamic virtual nozzle for generation of microscopic droplet streams,” *J. Phys. Appl. Phys.*, vol. 41, no. 19, p. 195505, Oct. 2008.
- [5] K. R. Beyerlein *et al.*, “Ceramic micro-injection molded nozzles for serial femtosecond crystallography sample delivery,” *Rev. Sci. Instrum.*, vol. 86, no. 12, p. 125104, Dec. 2015.
- [6] R. Zahoor, G. Belšak, S. Bajt, and B. Šarler, “Simulation of liquid micro-jet in free expanding high speed co-flowing gas streams,” *Microfluid. Nanofluidics*, vol. 22, no. 8, p. 87, 2018.
- [7] G. Nelson *et al.*, “Three-dimensional-printed gas dynamic virtual nozzles for x-ray laser sample delivery,” *Opt. Express*, vol. 24, no. 11, p. 11515, 2016.
- [8] T. Si, F. Li, X.-Y. Yin, and X.-Z. Yin, “Modes in flow focusing and instability of coaxial liquid–gas jets,” *J. Fluid Mech.*, vol. 629, p. 1, 2009.
- [9] D. Erickson, “Towards numerical prototyping of labs-on-chip: modeling for integrated microfluidic devices,” *Microfluid. Nanofluidics*, vol. 1, no. 4, pp. 301–318, Oct. 2005.
- [10] M. A. Herrada, A. M. Gañán-Calvo, A. Ojeda-Monge, B. Bluth, and P. Riesco-Chueca, “Liquid flow focused by a gas: Jetting, dripping, and recirculation,” *Phys. Rev. E*, vol. 78, no. 3, p. 036323, Sep. 2008.
- [11] R. Zahoor, S. Bajt, and B. Šarler, “Influence of Gas Dynamic Virtual Nozzle Geometry Micro-Jet Characteristics,” *Int. J. Multiph. Flow*, vol. 104, pp. 152–165, 2018.
- [12] R. Zahoor, S. Bajt, and B. Šarler, “Numerical investigation on influence of focusing gas type on liquid micro-jet characteristics,” *Int. J. Hydromechatronics*, vol. 1, no. 2, pp. 222–237, 2018.
- [13] J. U. Brackbill, D. B. Kothe, and C. Zemach, “A continuum method for modeling surface tension,” *J. Comput. Phys.*, vol. 100, no. 2, pp. 335–354, Jun. 1992.
- [14] H. G. Weller, G. Tabor, H. Jasak, and C. Fureby, “A tensorial approach to computational continuum mechanics using object-oriented techniques,” *Comput. Phys.*, vol. 12, no. 6, p. 620, 1998.
- [15] H. G. Weller, “A new approach to VOF-based interface capturing methods for incompressible and compressible Flow,” *Tech. Rep.*, no. May, p. 13, 2008.
- [16] R. Courant, K. Friedrichs, and H. Lewy, “On the partial difference equations of mathematical physics,” *IBM J. Res. Dev.*, vol. 11, no. 2, pp. 215–234, Mar. 1967.